28 p

[redacted]

43

MTP-AERO-63-73
October 23, 1963

X64 12766

Code 2D

# GEORGE C. MARSHALL SPACE FLIGHT CENTER

**HUNTSVILLE, ALABAMA**

CLASSIFICATION CHANGE
TO - UNCLASSIFIED
By authority of [redacted] E.O. 11652
Changed by L. Shirley Date 12-18-73

NASA TM X-54678

## RIGID BODY CONTROL STUDY FOR SA-5 (U)

By

E. L. Sullivan   23 Oct. 1963   28 p   refs

"Available to U.S. Government Agencies and U. S. Government Contractors Only"

~~GROUP 4
Downgraded at 3 year intervals; declassified after 12 years~~

Confidential rept GP-4

~~FOR INTERNAL USE ONLY~~

**NATIONAL AERONAUTICS AND SPACE ADMINISTRATION**

(NASA-TM-X-54678) RIGID BODY CONTROL STUDY FOR SA-5 (NASA) 28 p

N74-71603

Unclas
00/99 29626

[redacted]

MSFC - Form 523 (Rev. November 1960)

GEORGE C. MARSHALL SPACE FLIGHT CENTER

MTP-AERO-63-73

# RIGID BODY CONTROL STUDY FOR SA-5

By E. L. Sullivan

12766

A


(U) ABSTRACT

This report presents a study of the rigid body control of the SA-5 vehicle for the final flight trajectory. A wind restriction of 62.5 meters per second is imposed on the vehicle flight due to structural considerations. This wind restriction for the maximum dynamic pressure time of flight gives a launch probability of approximately 96% for the month of December. Use of the latest structural limitations and the 105° flight azimuth winds made the wind restrictions less severe and improved the launch probability over the last study presented.


uncl.

AUTHOR

[redacted]

GEORGE C. MARSHALL SPACE FLIGHT CENTER

MTP-AERO-63-73

October 23, 1963

# RIGID BODY CONTROL STUDY FOR SA-5 (U)

by

E. L. Sullivan

G[illegible] 4
Downgr[illegible] year intervals;
declassif[illegible] 12 years

FLIGHT MECHANICS BRANCH
AERO-ASTRODYNAMICS LABORATORY

[redacted]

(U) TABLE OF CONTENTS

# (U) LIST OF ILLUSTRATIONS

GEORGE C. MARSHALL SPACE FLIGHT CENTER

MTP-AERO-63-73

# RIGID BODY CONTROL STUDY FOR SA-5

By E. L. Sullivan

## (U) SUMMARY

This report presents a study of the rigid body control of the SA-5 vehicle for the final flight trajectory. A wind restriction of 62.5 meters per second is imposed on the vehicle flight due to structural considerations. This wind restriction for the maximum dynamic pressure time of flight gives a launch probability of approximately 96% for the month of December. Use of latest data on structural limitations and 105° flight azimuth winds made the wind restrictions less severe and improved the launch probability over the last data published.

## I. (U) INTRODUCTION

Rigid body control requirements are investigated for the SA-5 vehicle. The study is conducted for the first stage flight time with emphasis on the maximum dynamic pressure region. Wind restrictions are established based on structural limitations of the vehicle.

# II. (C) DATA AND ASSUMPTIONS

## A. (C) VEHICLE DESCRIPTION

The first stage propulsion system of the SA-5 vehicle consists of eight modified H-1 engines rated at 188k pounds thrust per engine at sea level. The second stage (S-IV) of the SA-5 vehicle is propelled by six Pratt and Whitney engines which develop 15k pounds thrust each under vacuum conditions. Pertinent performance data are:

First Stage

| | | | |
|---|---|---|---|
| Liftoff Mass............................. | 509665.5 | kg | 1,123,620 lbs |
| Thrust (sea level) (uncanted)........... | 6690125 | N | 1,504,000 lbs |
| Specific Impulse (sea level) (uncanted).. | 256 | sec | |
| Total Propellants (LOX/RP-1) (Mass)...... | 385553.6 | kg | 850,000 lbs |

Second Stage

| | | | |
|---|---|---|---|
| Liftoff Mass............................. | 62911.5 | kg | 138,696 lbs |
| Thrust (vacuum).......................... | 400339.95 | N | 90,000 lbs |
| Specific Impulse (vacuum)................ | 429.5 | sec | |
| Total Propellants ($H_2/O_2$) (Mass)......... | 45313.4 | kg | 99,899 lbs |

Payload

| | | | |
|---|---|---|---|
| Orbital Payload (Mass).................. | 8288.1 | kg | 18,272 lbs |

## B. (C) TRAJECTORY INFORMATION

This control study is based on the booster propelled flight phase of the SA-5 vehicle. A brief description of the flight history for the first stage powered flight is given in Table 1. The first stage powered flight is based on nominal eight engine booster operation using a "wind biased" tilt program. The wind used for the tilt biasing is the median December wind shown on Figure 5.

## C. (C) AERODYNAMIC AND STRUCTURAL DATA

The histories of the motion of the center of gravity (CG) and center of pressure (CP) over flight time are shown on Figure 1. This time history of the motion of the CG and CP shows the vehicle to be aerodynamically stable; i.e., the CG is forward of the CP, from approximately 48 seconds to 57 seconds of flight time when the velocity is around Mach 1. The slope of the normal force coefficient as a function of flight time is also shown on this same Figure 1. Shown on Figure 2 is the pitch moment of inertia as a function of flight time for the SA-5 vehicle. Figure 3 gives the dynamic pressure (q) over flight time for the powered phase of the booster flight. Due to structural considerations, angle of attack limitations are imposed on the flight of the SA-5 vehicle as a function of the dynamic pressure. This limitation is required because of the structural strength of the aft skirts on the fuel tanks. A picture of this area is shown on Figure 4.

D. (C) WIND ASSUMPTIONS

The wind disturbances used in this analysis are based on the 1, 2, and 3 sigma confidence level winds for the month of December on a 105° flight azimuth. These wind profiles are shown on Figure 6. The wind shears and embedded gusts used are based on the 99% confidence level.

The application of the wind disturbance to the vehicle is as follows. In order to obtain initial conditions for the control study, it is assumed that there is no wind and the vehicle is flying the "wind biased" tilt program during the booster flight phase. The initial angle of attack when there is no wind is shown on Figure 7 as a function of flight time. The control coefficients for each time point studied are obtained from this trajectory and are held constant for the wind application. The wind shears in the 10-14 km region are applied over a 5 km altitude layer increasing with altitude to .09 (m/s)/m until the wind profile magnitude is attained. In Reference 1 different confidence level wind data are given in terms of the wind speed change for certain altitude "scale-distances" for particular altitude layers and wind shear data for this same altitude layer. In this study certain wind speed changes are assumed and the associated wind gradient is obtained from Reference 1. From this data and the vehicle rate of change of altitude, the time of build-up for the wind speeds is determined, that is $t_B = (W_{max}/\dot{Y})(1/(\partial w/\partial y))$ where $W_{max}$ is the magnitude of the wind speed, $\dot{Y}$ is the vehicle rate of change of altitude and $\partial w/\partial y$ is the associated wind gradient. Digital computers are then used with the wind building up to the assumed wind speed in the time determined by the above equation. Embedded gusts are applied at the top of this synthetic wind build-up for maximum effect from the gusts. A typical wind build-up profile is shown on Figure 8 with the added gust effects for the 10-14 km altitude layer. These embedded gusts of 9 m/s applied over a wave length ($\lambda$) of 300 meters are described in Reference 2. The effects of the shear and gusts are combined with the effects of the steady state wind as described in Reference 3, i.e., the angle of attack for a steady state wind is increased by the square root of the sum of the squares of the shear and gust effects ($\alpha_{total} = \alpha_{ss} + \sqrt{\alpha_{sh}^2 + \alpha_G^2}$). The same criteria is used in obtaining the gimbal angle ($\beta$) and other control data.

[redacted]

## III. (C) ANALYSIS

The aerodynamic restoring moment coefficient ($C_1$) and control moment coefficient ($C_2$) as a function of flight time are shown on Figure 9. The ratio of the aerodynamic restoring moment coefficient and the control moment coefficient ($C_1/C_2$) is shown on Figure 10 as a function of flight time. This ratio reaches a local peak instability of -.07 at approximately 40 seconds, a peak positive stability of .13 at approximately 54 seconds, and then peak instability of -.33 at approximately 77 seconds.

A double sensing control system utilizing a missile-fixed accelerometer and attitude control is used in the pitch and yaw planes. The accelerometers are located in the instrument unit at station 1500. A second order differential equation for a mathematical simulation of the accelerometer and attitude filters is used. This simulation is good up to a frequency of approximately .6 cycles per second. The control gains ($a_o$, $g_2$) used are those furnished by M-ASTR (Reference 4) and are presented as a function of flight time on Figure 11.

Angle-of-attack ($\alpha$) peaks are shown on Figure 12 for the 1, 2, and $3\sigma$ winds for the 105° flight azimuth for the month of December during the high dynamic pressure time of flight, i.e., from the 60th to the 75th second of flight time. The disturbances used to obtain these peaks other than the December winds include the 99% probability shears and gusts, the 95% probability for $C_1$ and $C_2$ variations (Reference 5), and a 10% variation for control gains (Reference 6). The effects of these variations are all added by the root sum square method. Shown also on Figure 12 is angle-of-attack limit due to structural loads from 65 to 75 seconds. Limits for other time points are not available. However, based on the data available, the most critical time point due to structural loads is around the 70th second of flight.

Figure 13 shows the gimbal angle ($\beta$) peaks for the same time of flight as above with the same disturbances. The gimbal angle requirement for the three winds is less than 4 degrees which is well within the 7 degree swivel capability of the SA-5 vehicle.

## IV (U) CONCLUSIONS

Figure 14 shows the angle-of-attack as a function of wind speed for the most critical time point (t=70 sec). It is shown here that the 5 degree limit for this time point gives a wind restriction of approximately 51.5 m/s for the unbiased tilt program and a wind restriction of approximately 62.5 m/s for the biased tilt program. Figure 15 shows the 105° flight azimuth winds as a function of percent probability of occurrence for

[redacted]

several months of the year. Using this figure and wind restriction of 51.5 m/s gives a probability of launch of approximately 87.5% for the unbiased tilt program. Using the wind restriction of 62.5 m/s gives a probability of launch of approximately 96% for the "wind biased" tilt program.

The improvement in launch probability is due mainly to new information on the structural limitations. Previously the 5° angle-of-attack was used for all the high dynamic pressure region making the time point of approximately 63 seconds the most critical and therefore making the wind restriction more severe. Also the use of flight azimuth wind statistics for December rather than scalar wind statistics makes the launch probability percentage higher.

## (C) TABLE 1

## SA-5 PROPELLED FLIGHT TRAJECTORY

8 x 188k Engines — $F$ = 1,504,000 lb.(Uncanted) — $W_o$ = 1,123,620 lb.
850,000 lb.Prop.Consumption — $I_{sp}$ = 256 sec. (Uncanted) — $W_e^o$ = 373,620 lb.

| Time (sec) | Ground Distance (km) | Altitude (km) | Velocity (m/sec) | Path Angle (deg) | Acceleration v Dot M/sec$^2$ | Mach |
|---|---|---|---|---|---|---|
| 0 | 0 | 0.03 | 0 | 0 | -2.81 | 0 |
| 20 | 0 | 0.81 | 84.3 | 0.58 | 5.13 | 0.25 |
| 40 | 0.46 | 3.62 | 209.4 | 16.53 | 7.59 | 0.62 |
| 60 | 2.79 | 8.99 | 382.8 | 28.64 | 9.70 | 1.20 |
| 65 | 3.81 | 10.75 | 434.4 | 31.31 | 10.95 | 1.39 |
| 70 | 5.06 | 12.70 | 492.9 | 33.86 | 12.50 | 1.63 |
| 75 | 6.57 | 14.85 | 559.9 | 36.35 | 14.32 | 1.90 |
| 80 | 8.38 | 17.21 | 635.5 | 38.87 | 16.32 | 2.19 |
| 100 | 19.84 | 29.09 | 1048.1 | 48.06 | 24.94 | 3.46 |
| 120 | 40.60 | 45.52 | 1645.3 | 54.72 | 35.35 | 4.93 |
| 140 | 74.92 | 67.31 | 2504.9 | 60.16 | 52.13 | 8.39 |
| 142.6 | 80.69 | 70.61 | 2595.9 | 60.64 | 24.14 | 9.00 |
| 147 | 90.77 | 76.26 | 2700.9 | 61.34 | -1.51 | 9.98 |

| Time (sec) | Mass | | Dynamic Pressure N/m$^2$ | Thrust | | Drag N |
|---|---|---|---|---|---|---|
| | lbs. | kg | | lbs. | N | |
| 0 | 1123620 | 509666 | 0 | 1497503 | 6661226 | 44130 |
| 20 | 1005264 | 455980 | 3903 | 1548758 | 6889221 | 90074 |
| 40 | 886214 | 401980 | 17887 | 1600411 | 7118981 | 306350 |
| 60 | 767147 | 347972 | 32911 | 1660577 | 7386614 | 1024981 |
| 65 | 737290 | 334429 | 34382 | 1674248 | 7447425 | 991609 |
| 70 | 707439 | 320889 | 34667 | 1687107 | 7504627 | 890218 |
| 75 | 677582 | 307346 | 33382 | 1698276 | 7554308 | 737509 |
| 80 | 647740 | 293810 | 29979 | 1706634 | 7591485 | 570855 |
| 100 | 529061 | 239978 | 11582 | 1722165 | 7660573 | 120583 |
| 120 | 410549 | 186222 | 2579 | 1717771 | 7641028 | 16691 |
| 140 | 292249 | 132562 | 461 | 1696462 | 7546237 | 1147 |
| 142.6 | 280997 | 127458 | 314 | 826374 | 3675895 | 647 |
| 147 | 267972 | 121550 | 147 | 84001 | 373653 | 196 |

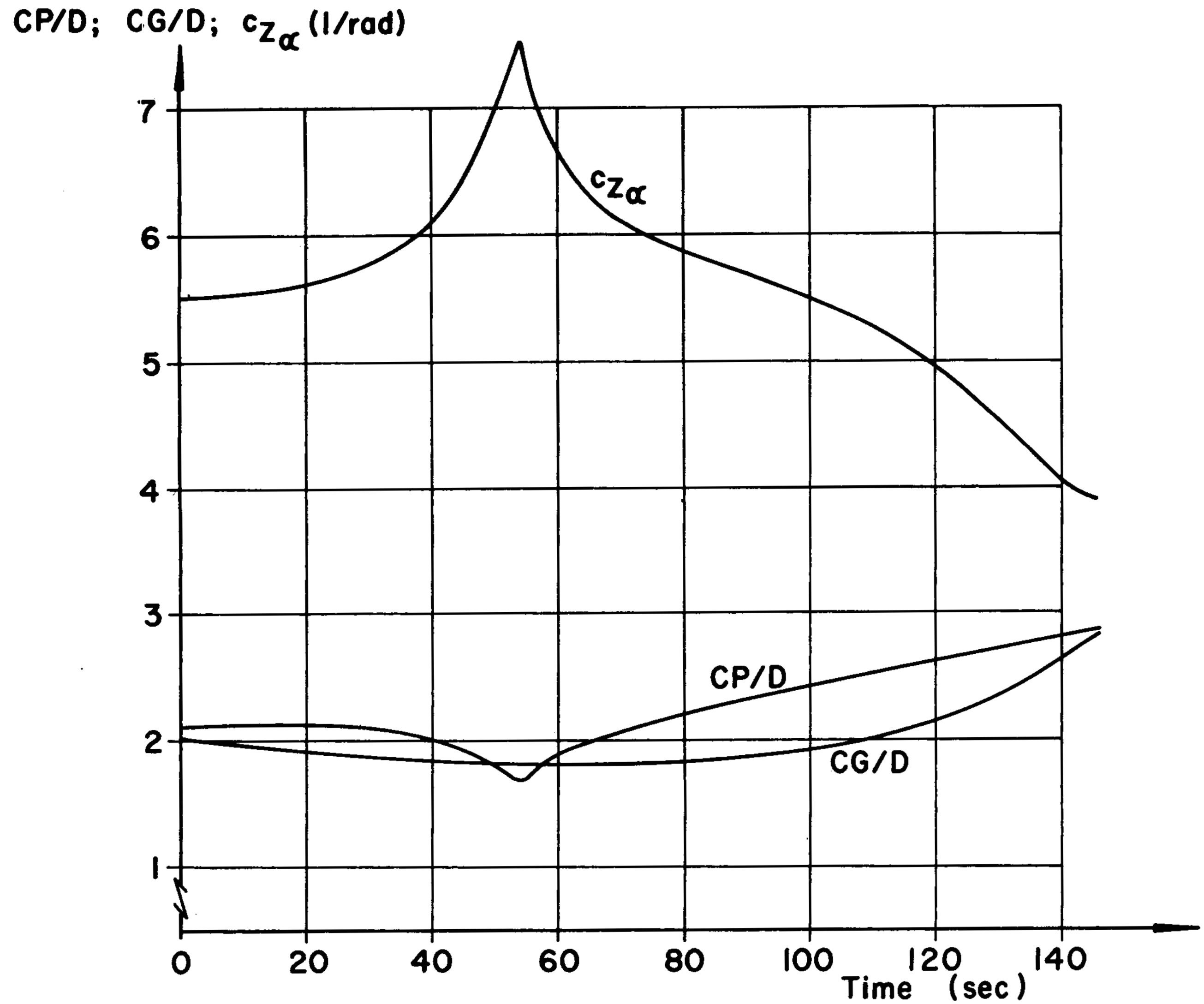


FIG. I. VARIATION OF CENTER OF PRESSURE (CP/D), CENTER OF GRAVITY (CG/D) AND SLOPE OF LIFT COEFFICIENT ($c_{Z_\alpha}$) WITH FLIGHT TIME

[redacted]

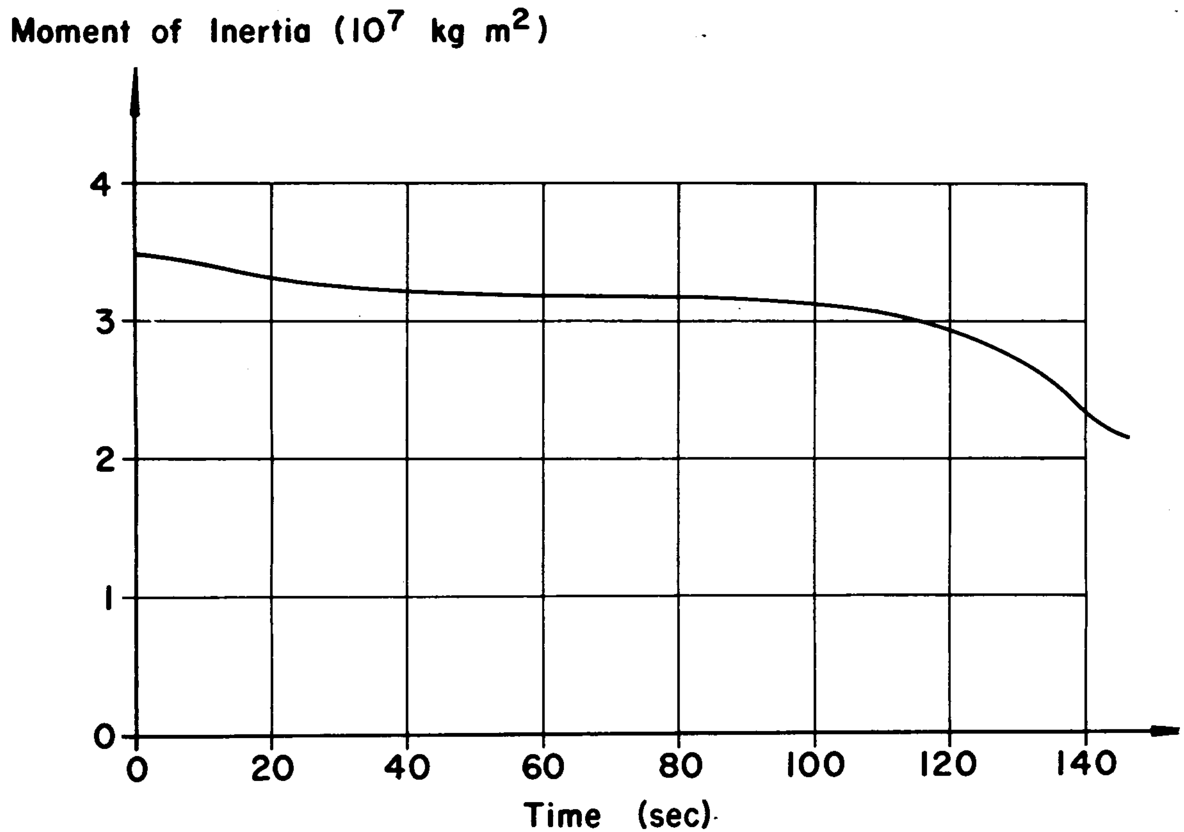


FIG. 2. MASS MOMENT OF INERTIA IN PITCH VERSUS FLIGHT TIME

[redacted]

[redacted]



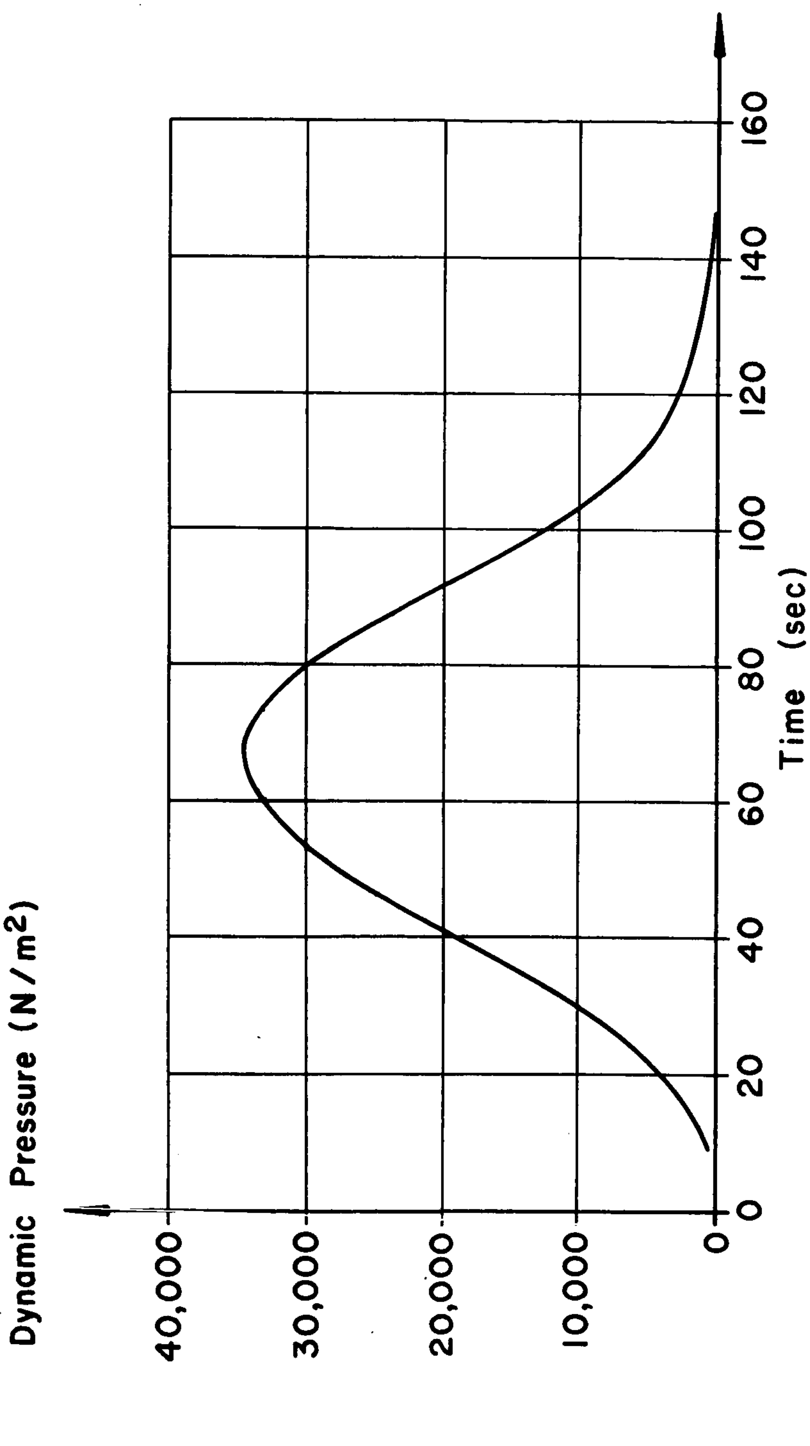


FIG. 3. DYNAMIC PRESSURE VERSUS FLIGHT TIME

[redacted]

[redacted]

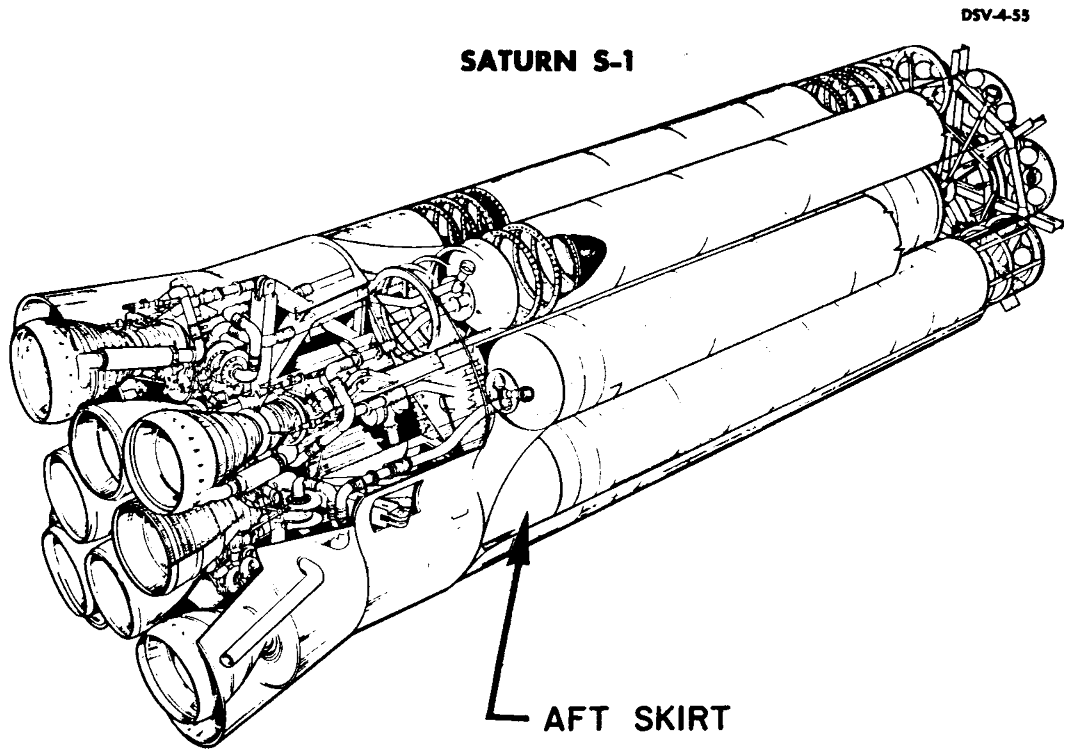


FIG. 4. DRAWING OF SA-5 SHOWING AFT SKIRTS ON FUEL TANKS

[redacted]

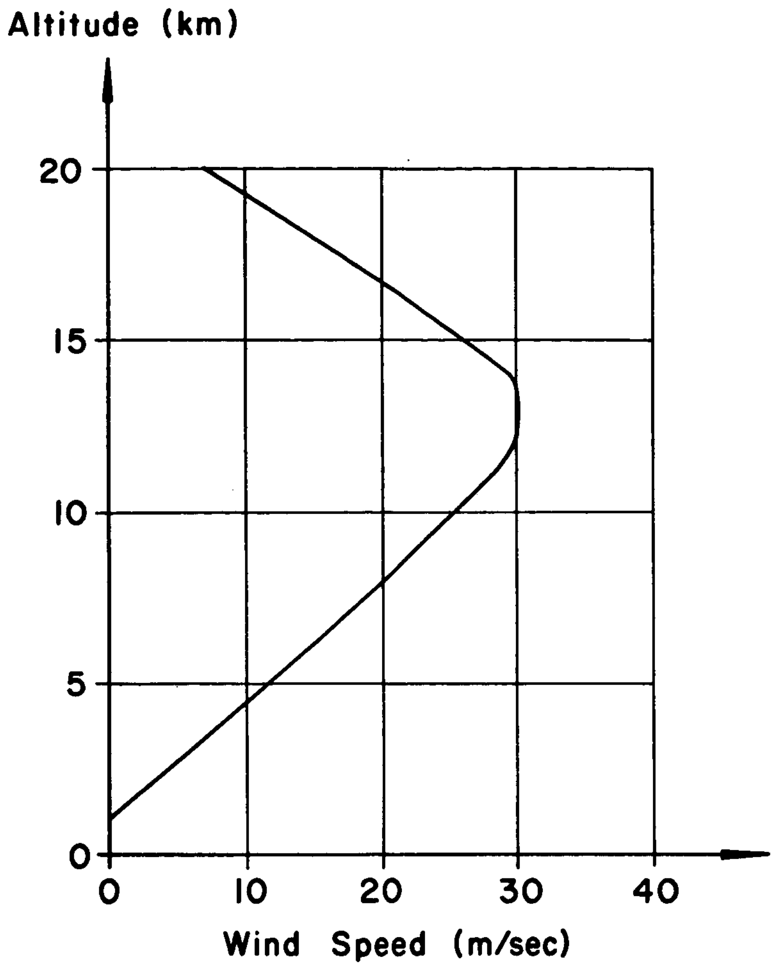


FIG. 5. MEDIAN DECEMBER WIND PROFILE ENVELOPE FOR 105° FLIGHT AZIMUTH

[redacted]

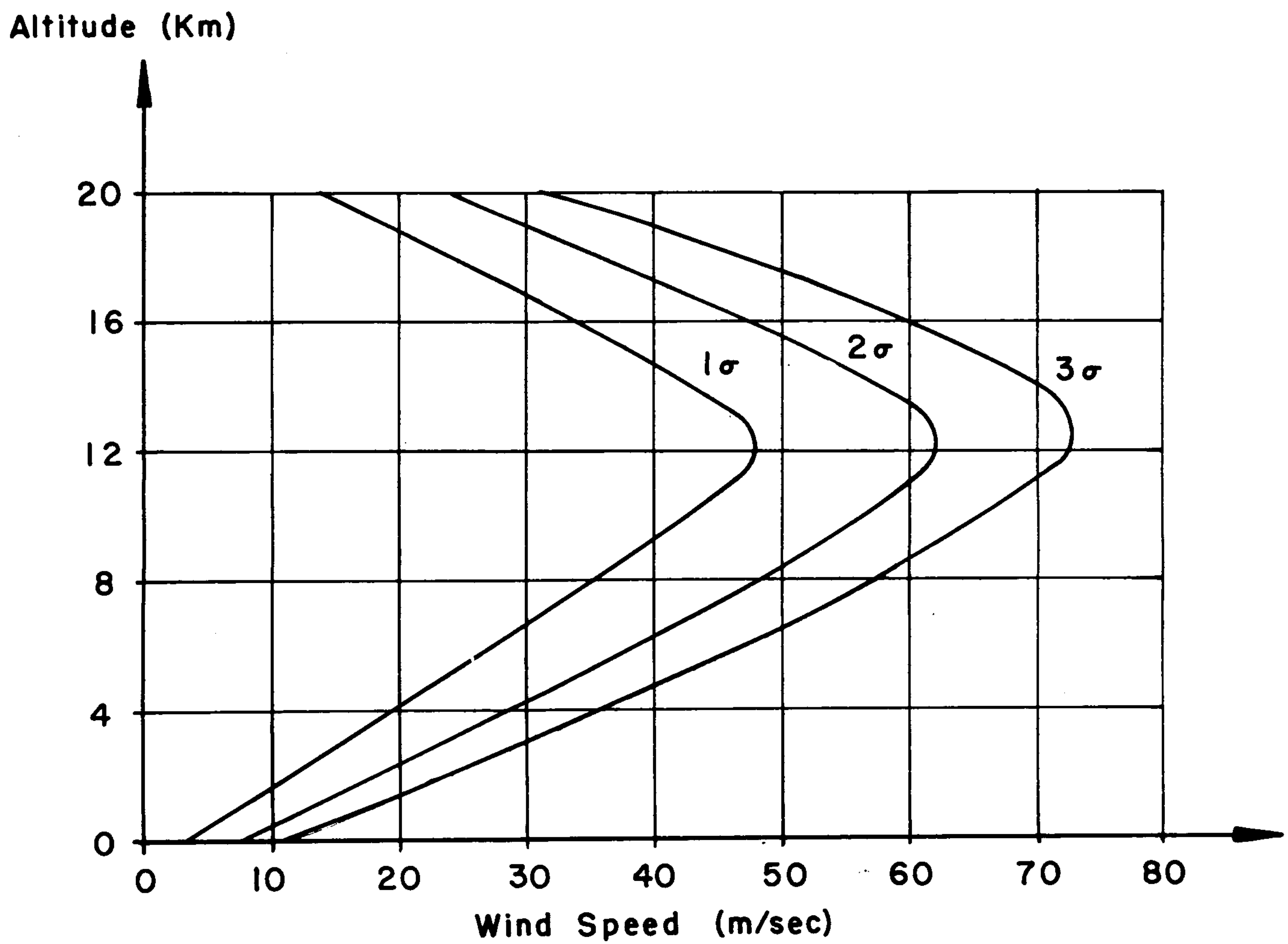


FIG. 6. WIND PROFILE ENVELOPES FOR DECEMBER FOR 105° FLIGHT AZIMUTH

[redacted]

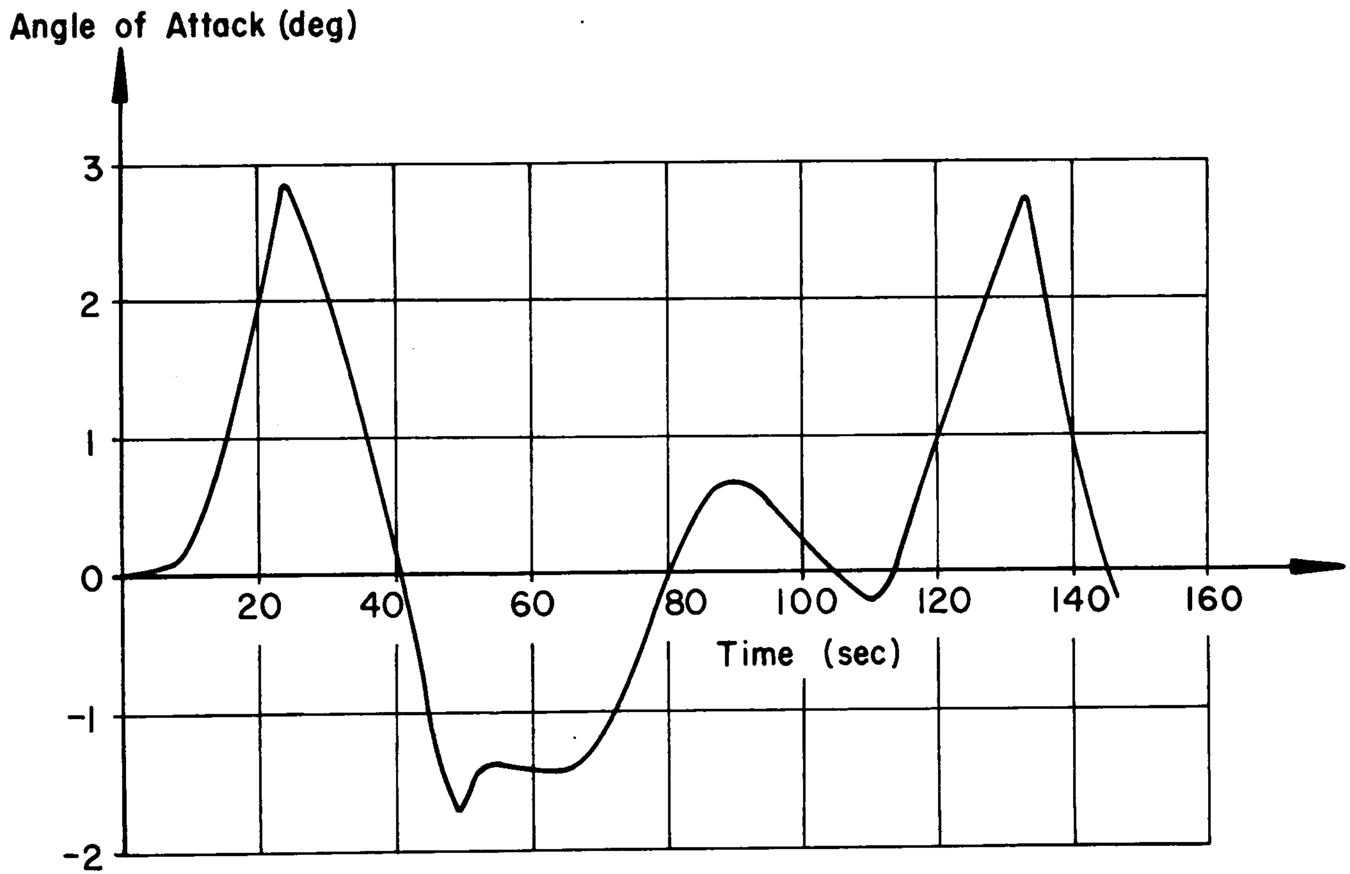


FIG. 7. ANGLE OF ATTACK ($\alpha$) VERSUS FLIGHT TIME "WIND BIASED" TILT PROGRAM WITH NO WIND

[redacted]

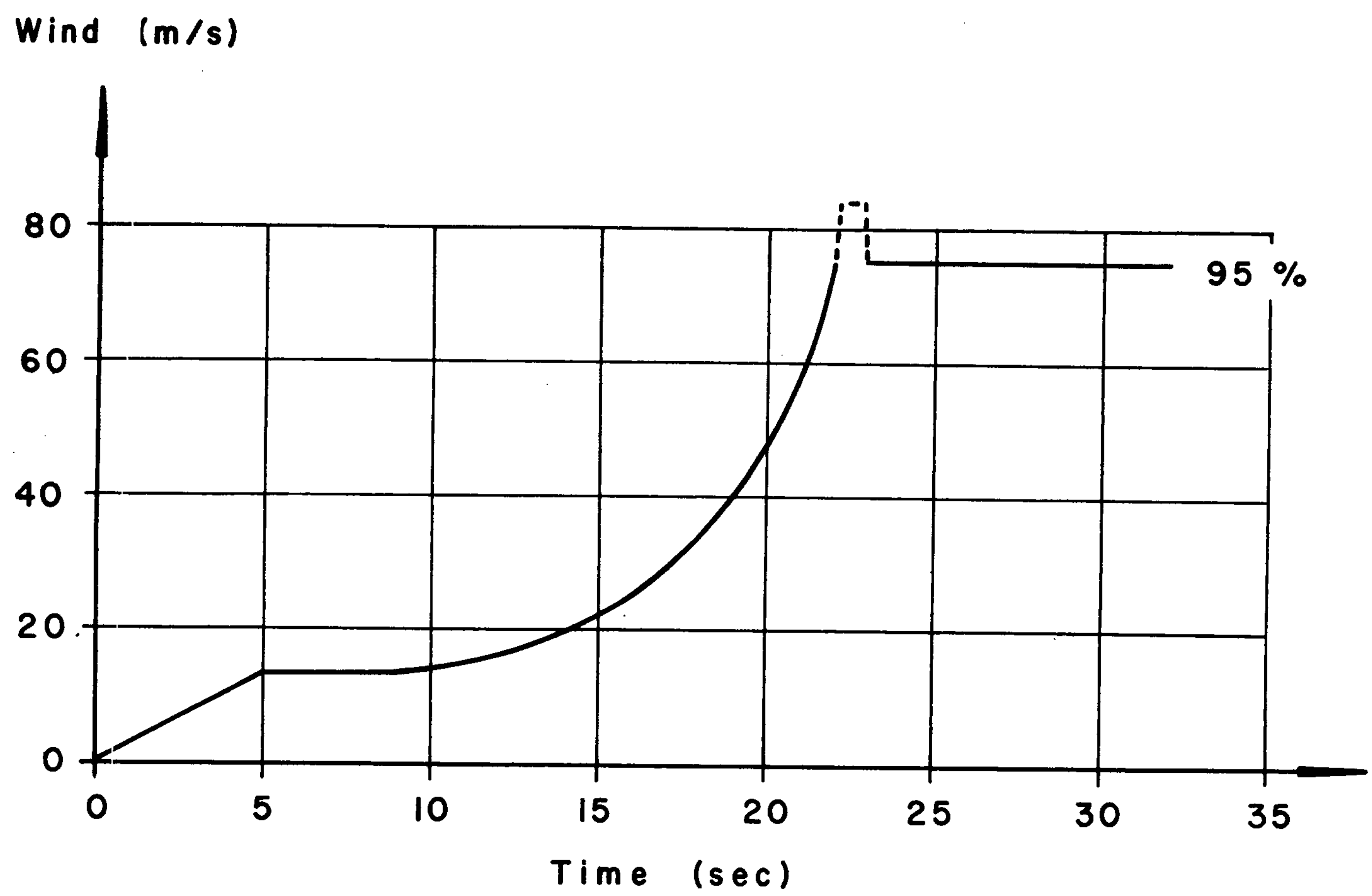


FIG. 8. TYPICAL SYNTHETIC WIND PROFILE FOR 10-14 KM ALTITUDE

[redacted]

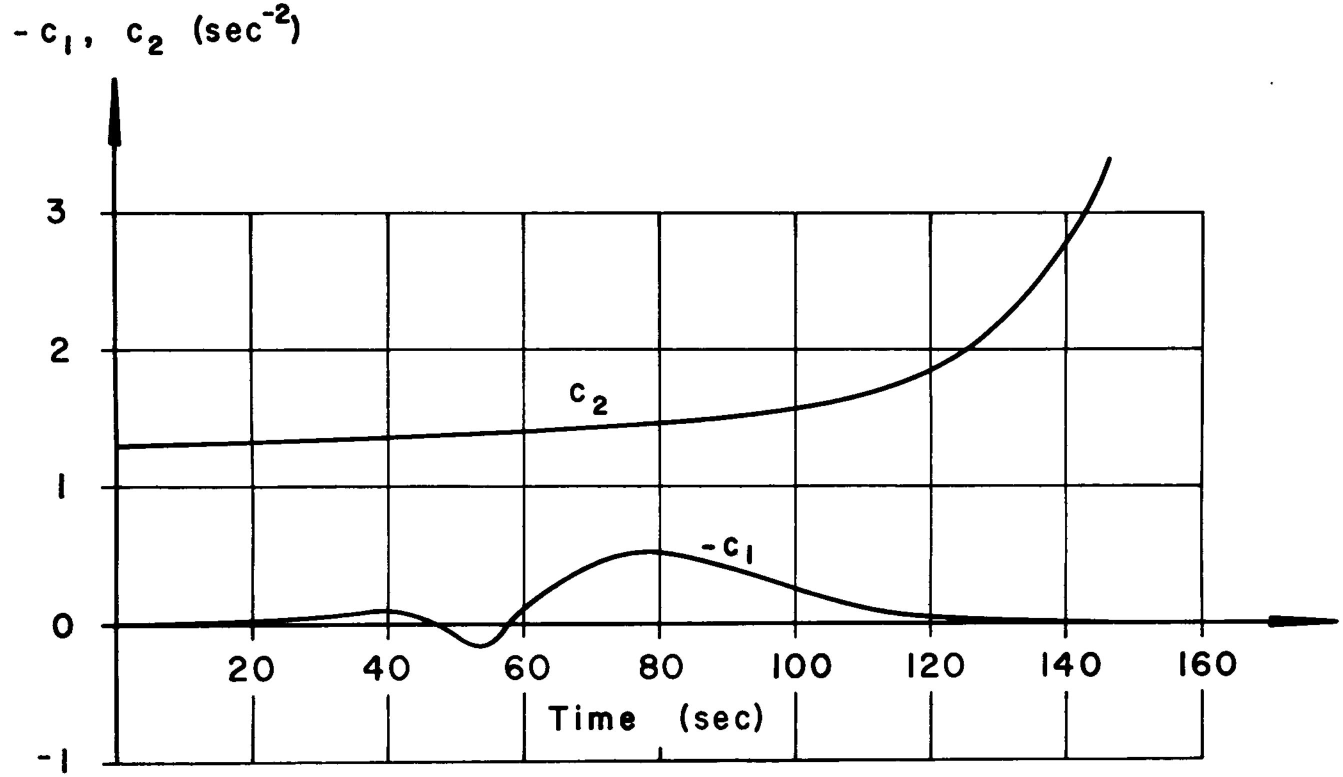


FIG. 9. AERODYNAMIC RESTORING MOMENT COEFFICIENT $c_1$ AND CONTROL MOMENT COEFFICIENT $c_2$ VERSUS FLIGHT TIME

[redacted]

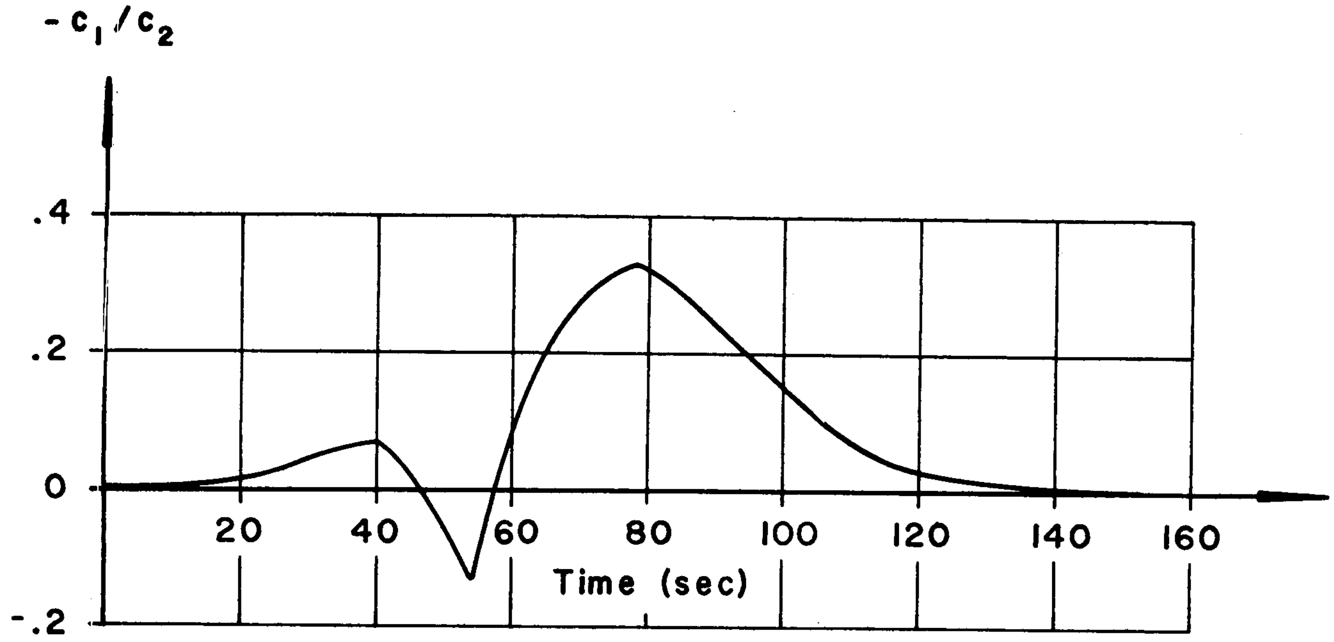


FIG. 10. RATIO OF AERODYNAMIC RESTORING MOMENT COEFFICIENT $c_1$ TO CONTROL MOMENT COEFFICIENT $c_2$ VERSUS FLIGHT TIME

[redacted]

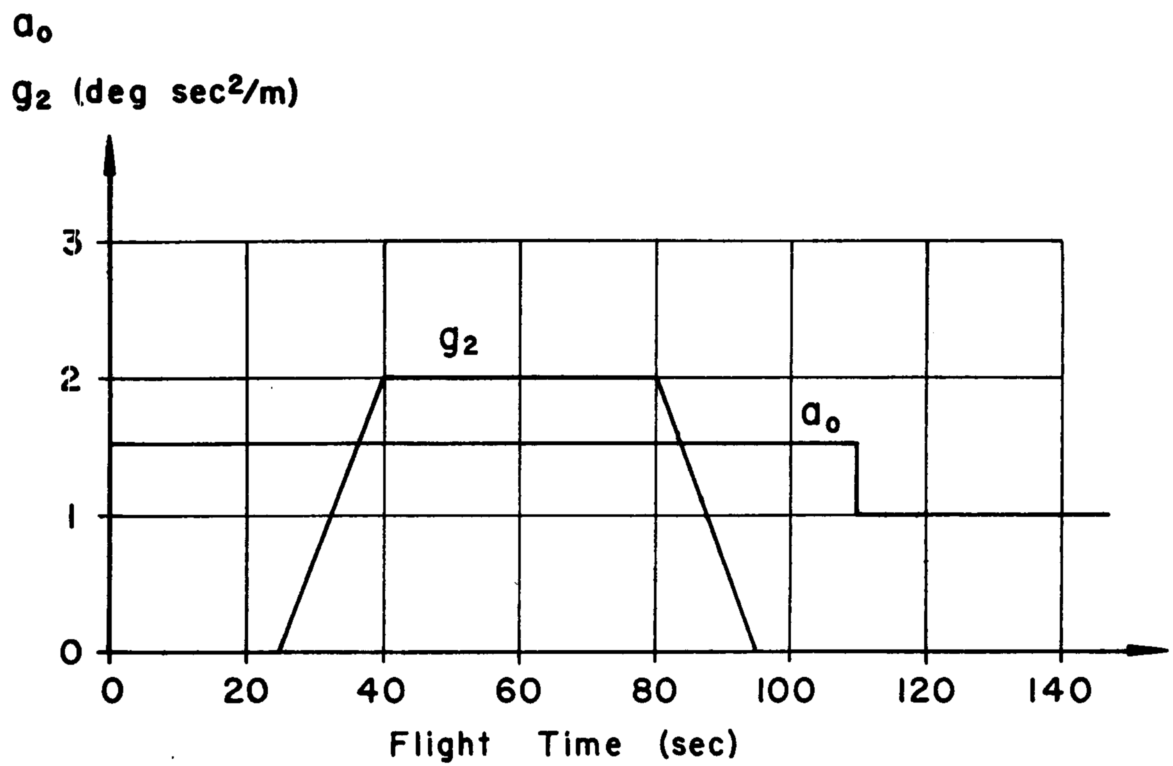


FIG. 11. CONTROL GAINS VERSUS FLIGHT TIME

[redacted]

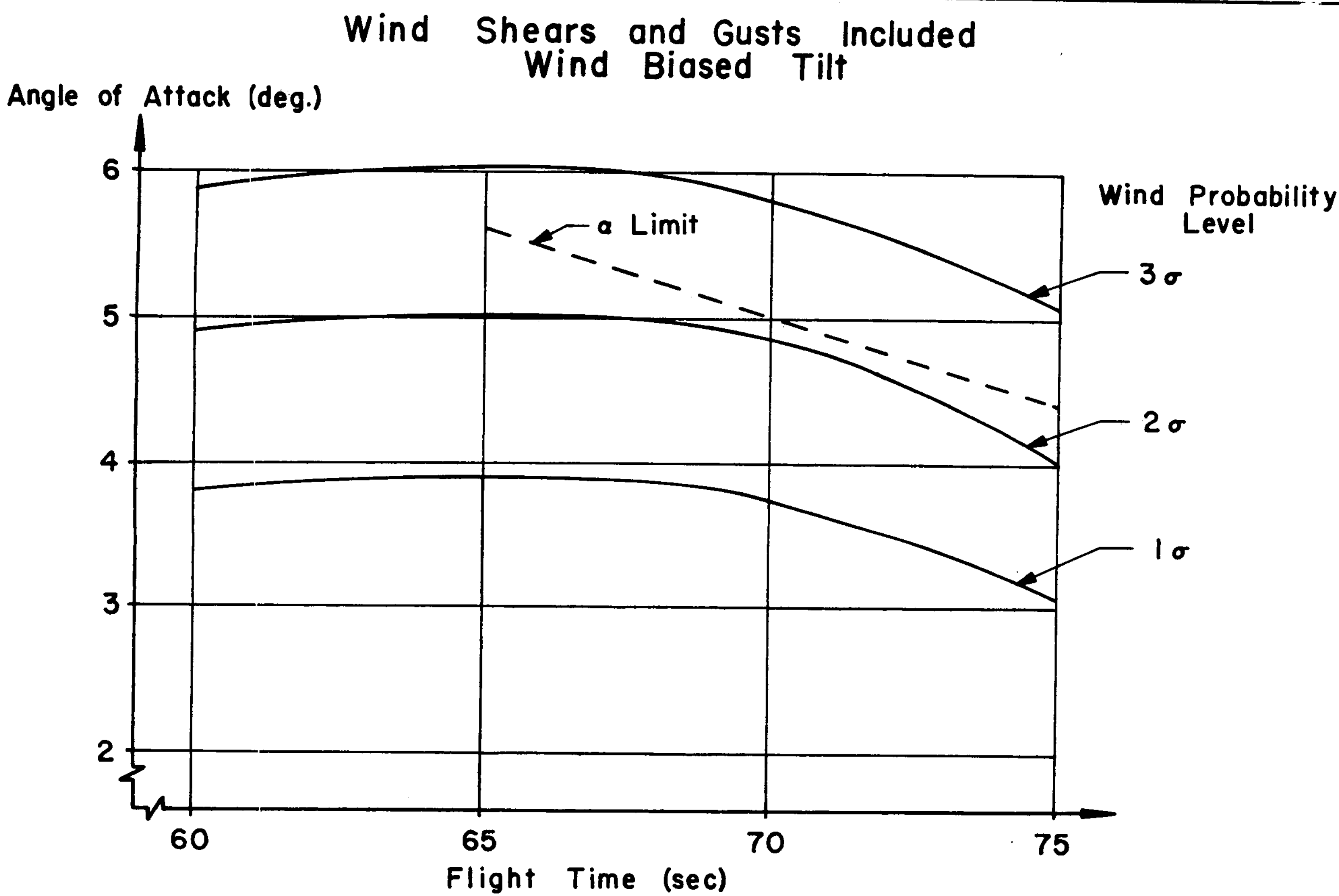


FIG. 12. Maximum Angle of Attack versus Flight Time For Three December Wind Magnitudes

[redacted]

Wind Shears and Gusts Included
Wind Biased Tilt

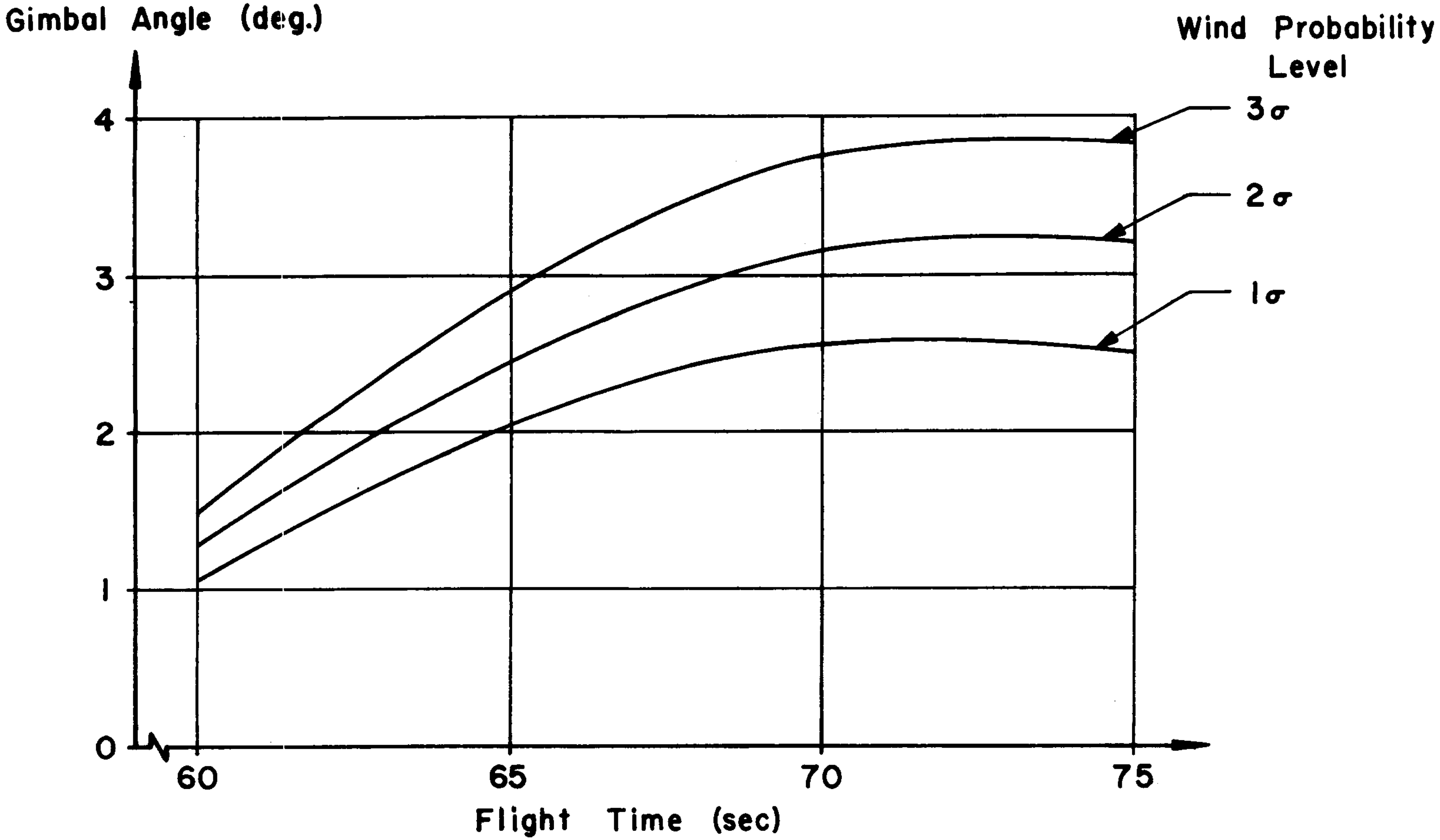


FIG. 13. Maximum Gimbal Angle versus Flight Time For Three December Wind Magnitudes

[redacted]

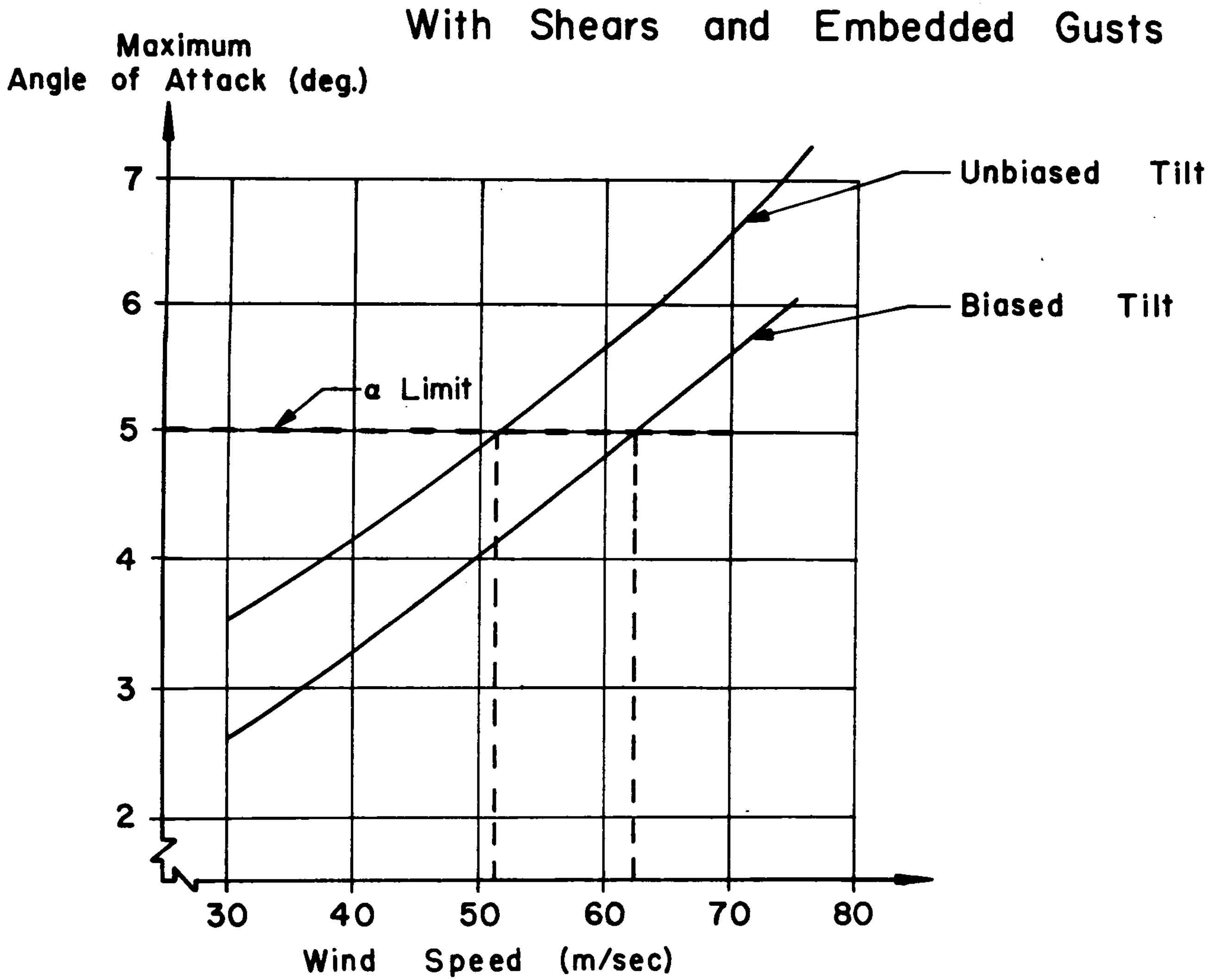


FIG.14. Maximum Angle of Attack versus Wind Speed In Maximum Pressure Region (t=70 sec)

[redacted]

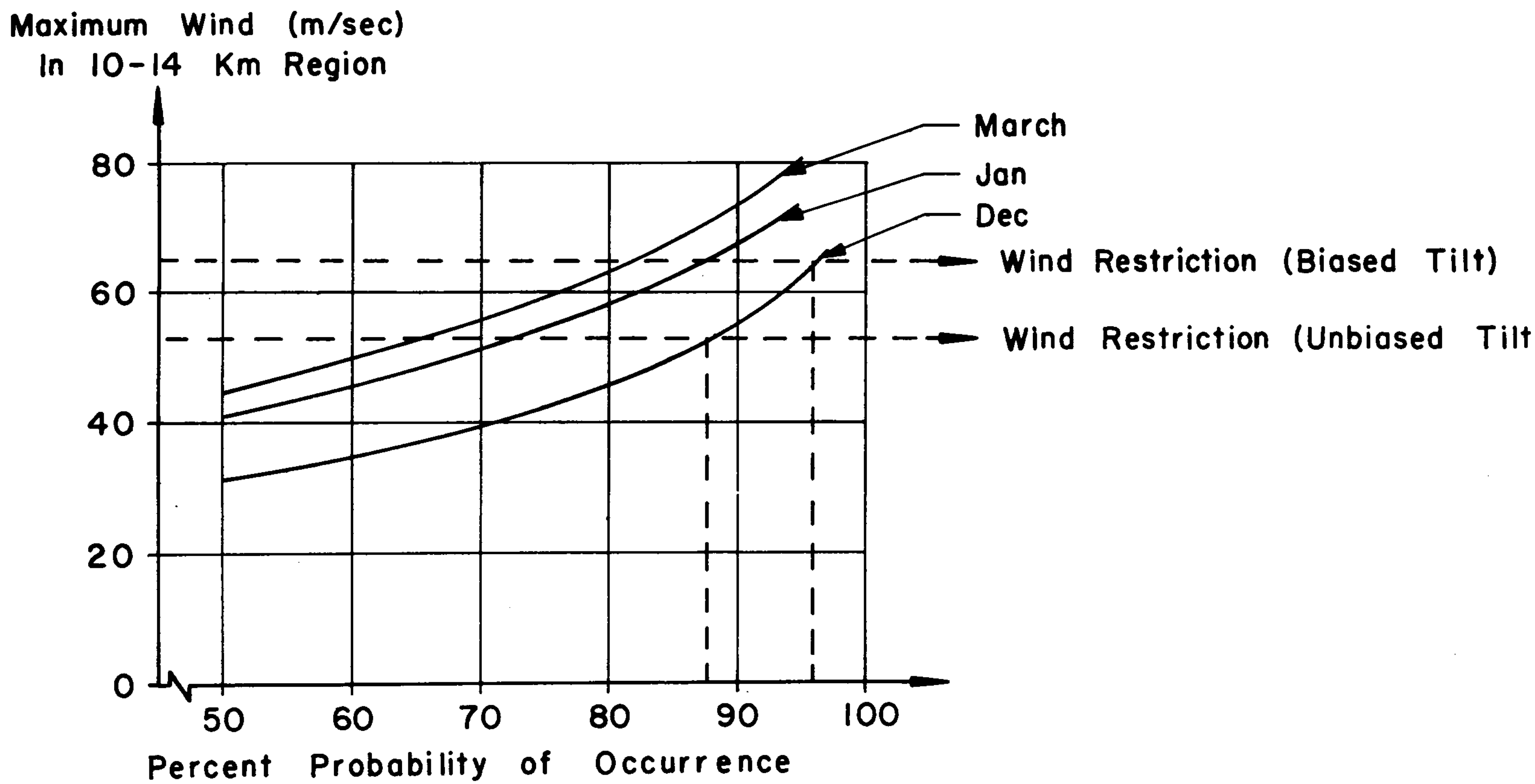


FIG. 15. PROBABILITY OF OCCURRENCE OF VARIOUS WIND LEVELS FOR DIFFERENT MONTHS OF THE YEAR FOR 105° FLIGHT AZIMUTH

## REFERENCES


1. Wind Shears vs Wind Speed for Determining Wind Velocity Limits in Control Studies where Maximum Vehicle Response Occurs between 7 and 15 km.

2. Revision of Natural Environmental Design Criteria, in Flight Wind Conditions, Saturn C-I, Block II Vehicle by G. Daniels, M-AERO-G-35-62, October 19, 1962.

3. Saturn and Other MSFC Launch Vehicle Rigid Body Control and Structural Response Studies by W. W. Vaughan, M-AERO-G-61-63, June 14, 1963.

4. Saturn SA-5 Control Gains and Shaping Networks by Mr. Blackstone, Flight Dynamics Branch, M-ASTR-F, July 1, 1963.

5. Saturn Control Factors for Saturn I SA-5 Vehicle by Larry K. Donehoo, Aero Internal Note No. 29-63, June 10, 1963.

6. Saturn SA-5 Navigation Specifications, Accelerometer Angle-of-Attack Control by D. R. Scott, R-ASTR-N-496, July 15, 1963.

APPROVAL

MTP-AERO-63-73

RIGID BODY CONTROL STUDY FOR SA-5

By

E. L. Sullivan

CONCURRENCE:

L. O. Stone

L. O. STONE
Chief, Flight Mechanics Branch

Lewis L. McNair

L. L. McNAIR
Chief, Projects Office

Speer

F. A. SPEER
Chief, Flight Evaluation and Operations Studies Division

Geissler

E. D. GEISSLER
Director, Aero-Astrodynamics Laboratory

DISTRIBUTION

Dr. von Braun, DIR

Mr. Rees, DEP-T

Mr. Gorman, DEP-A

Dr. Geissler, R-AERO-DIR
Mr. Jean, R-AERO-DIR
Mr. Dahm, R-AERO-A
Mr. Wilson, R-AERO-A
Mr. Linsley, R-AERO-A
Mr. Holderer, R-AERO-A
Mr. Horn, R-AERO-D
Mr. Baker, R-AERO-D
Mr. Winch, R-AERO-D
Dr. Speer, R-AERO-F (2)
Mr. Lindberg, R-AERO-F
Mr. Stone, R-AERO-F
Mr. Sheats, R-AERO-F
Mr. Hardage, R-AERO-F
Mr. Sullivan, R-AERO-F (5)
Mr. McNiel, R-AERO-F
Dr. Hoelker, R-AERO-P
Mr. McNair, R-AERO-PS
Mr. Reed, R-AERO-TS
Mr. Cummings, R-AERO-TS
Mr. W. Vaughan, R-AERO-Y
Mr. Teague, R-AERO-PS (7)
Mr. Ryan, R-AERO-D

Dr. Hoelzer, R-COMP-DIR

Mr. Heimburg, R-TEST-DIR

Dr. Haeussermann, R-ASTR-DIR
Mr. Hoberg, R-ASTR-F
Mr. Blackstone, R-ASTR-F
Mr. Taylor, R-ASTR-F
Mr. Mink, R-ASTR-F
Mr. Mandel, R-ASTR-G
Mr. Blanton, R-ASTR-E
Mr. Hosenthien, R-ASTR-F
Mr. Moore, R-ASTR-G
Mr. Boehm, R-ASTR-M
Mr. Brandner, R-ASTR-TSJ (2)
Mr. Fichtner, R-ASTR-E

Dr. Mrazek, R-P&VE-DIR
Mr. Hellebrand, R-P&VE-DIR
Mr. Paul, R-P&VE-P
Mr. Mintz, R-P&VE-OR
Mr. Denton, R-P&VE-FS
Mr. Suber, R-P&VE-F
Mr. Schulze, R-P&VE-E
Mr. Kroll, R-P&VE-S
Mr. Showers, R-P&VE-S
Mr. Hunt, R-P&VE-S
Mr. Belew, R-P&VE-S
Mr. Hastings, R-P&VE-S
Mr. Palaoro, R-P&VE-V (2)

Mr. Grau, R-QUAL-DIR

Mr. Kuers, R-ME-DIR

Dr. Gruene, LVO-DIR
Mr. Hershey, LVO-E
Mr. Moser, LVO-G
Mr. Chambers, LVO-GA
Mr. Varnadoe, LVO-ET
Mr. Davidson, LVO-GE
Mr. Jenke, LVO-GE
Mr. Whiteside, LVO-GN
Mr. Williams, LVO-E
Mr. Gorman, LVO-M

Dr. Debus, LO-DIR
Dr. Knothe, LO-T
Mr. White, LO-I
Dr. Bruns, LO-ED
Mr. Moore, LO-T
Mr. Jelen, LO-T

MS-IP
MS-IPL (8)
MS-H
HME-P
PAT

Scientific and Technical Information
Facility (2)
ATTN: NASA Representative S-AK/RKT
P. O. Box 5700
Bethesda, Maryland